

Synchrotron Radiation in the Infrared and its Application for Solid State Investigations

P. Roy^a, P. Calvani^b, Y. L. Mathis^a, S. Lupi^{b,a}, B. Tremblay^a and A. Gerschel^{a,c}

^a *LURE, Bat. 209D, Orsay 91405, France*

^b *Dip. di Fisica - Univ. di Roma - P. A. Moro 2, 00185 Roma, Italy*

^c *CPMA, Bat. 490, Orsay 91405, France*

Received December 22, 1992; revised manuscript received March 9, 1993

The properties of synchrotron radiation in the domain of the infrared and far-infrared are reviewed and its advantages over conventional sources are discussed. The new infrared facility in Orsay (SIRLOIN), which is positioned on a wiggler, is described. A review of infrared optical experiments in solid state physics is presented, with emphasis on measurements where Infrared Synchrotron Radiation (IRSR) appears to provide major improvements over conventional spectroscopy. In particular, we discuss: I) studies of excitonic spectra in molecular crystals under pressure. II) shallow donor levels and insulating-to-metal transitions in semiconductors, III) investigations on anomalous Drude reflectivity in untwinned High- T_c superconductors, IV) gap determinations in thin superconducting single crystals.

I. Introduction

Radiation emerging from bending magnets in synchrotron and storage rings is increasingly utilised as a far-infrared source. Infrared synchrotron Radiation (IRSR) facilities are operating at the NSLS VUV in Brookhaven^[1] (U.S.A.) and on the UVSOR^[2] and SPring-8^[3] facilities (Japan). Further beamlines are under construction or testing in Daresbury (UK)^[4], at the MAX1 ring of Lund^[5] (Sweden), and again at Brookhaven. Indeed, such sources are by two or three orders of magnitude brighter than a black body emitter at 2000 K, at all infrared wavelengths. On the other hand, the total photon flux Φ (number of photon/second/unit bandwidth) is considerably greater than that emitted by a black body for wavelengths $\lambda > 100 \mu\text{m}$ only^[1,2]. Therefore, use of IRSR from bending magnets has been proven to be advantageous for measurements on small samples and/or in the 10000-100 μm (1-100 cm^{-1}) range. The gain in brightness in this spectral region has interest pertaining at numerous fundamental fields, as for example studies of excitation spectra in crystals under pressure, or determinations of the superconducting gap in thin single crystals as described further.

An alternative source of IRSR is a wiggler, which may present advantages in terms of flexibility, photon flux, and extraction optics. Such a choice has been done

at the Super-ACO ring of Orsay, where the infrared beamline SIRLOIN is now under final test^[6]. The calculated intensity of SIRLOIN, as explained in this paper, is significantly greater than that of a black body or of a bending magnet of the same ring, therefore extending the range of applications of synchrotron radiation. For example, the study of Drude anomalies in High- T_c superconductors requires untwinned crystals, which drastically limits their size, and a source with broad spectral range extending up to the mid-infrared.

In the first part of this paper we describe the beam line extraction system and optics, as well as the results of calculations of photon flux. In the second part we present a few experiments that have been or could be performed by IRSR, emphasizing its advantages with respect to conventional sources.

II. Calculation of infrared synchrotron radiation flux

II.a) Calculation of the photon flux from an undulator in the "wiggler mode"

Let us consider an undulator, U , of length L and magnet period Λ . It generates a static magnetic field

$$B(z) = B_0 \cos(2\pi z/\lambda_u) \quad (1)$$

where z varies from 0 to L along the axis of the undulator. When relativistic particles pass through U , they oscillate in the plane of the ring with an amplitude Δx which is comparable with the transverse dimension of the beam itself. At any point of the particle sinusoidal path, radiation is emitted tangentially to the trajectory. The resulting light beam propagates as a cone coaxial with the particle beam.

In the "undulator mode" the $2N$ magnets (N periods) of U can provide along the axis a very bright quasi-monochromatic photon beam, due to the occurrence of a N^2 enhancement factor. The enhancement is determined by the interference between electromagnetic fields emitted by the same particles along its trajectory (contributions from different particles add up incoherently). In the plane of the ring, the first harmonic wavelength λ_1 of such an undulator may be tuned by varying either the magnetic field B_0 and/or the charged particle energy

$$\lambda_1 = 13.056\lambda_u[1 + (K^2/2)]/E^2 \quad (2)$$

where λ_1 is given in \AA , A in cm, E is the particle energy in GeV, $K = 0.934 \lambda_u B_0$ is the deflection parameter and $\gamma = E/mc^2$.

On the other hand, whenever

$$\lambda_1 \gg \lambda$$

the coherence effects disappear, the photon flux is simply enhanced by a factor $2N$ and the undulator is used in the "wiggler mode".

In turn^[7], when measured off-axis equation (2) becomes:

$$\lambda_1 = 13.056\lambda_u[1 + (K^2/2) + \gamma^2\vartheta^2]/E^2. \quad (3)$$

Infrared synchrotron radiation is mainly collected off-axis and, as shown by Eq. (3), λ_1 rapidly increases with increasing ϑ . By introducing the parameters which hold for Super ACO^[6] ($\gamma = 1565.55$, $K = 6.9$, $\lambda_u = 12.9$ cm) into Eq. (3), one finds that the incoherence condition is fulfilled for any $A \ll 58.7 \mu\text{m}$ if $\vartheta = 30$ mrad. This result shows that in the infrared the radiation is incoherent, while coherence effects could in principle be observed in the far infrared region.

However, the observation of coherence is unlikely even at long wavelengths for the following reasons: I)

radiation is collected under a wide acceptance angle, thus causing a superposition of spectra with different λ_1 , according to (3); II) e.m. fields emitted at points separated by A , $2\lambda_u$, $3\lambda_u$, ... will be intercepted by the collecting mirrors under different angles, as those are placed at a finite distance from the undulator (approximately 1.5 m from the end of the undulator). This also considerably reduces spatial coherence.

From the above discussion we conclude that the incoherent "wiggler mode" may be assumed as valid in the present case. In order to calculate the total photon flux as a function of the radiation wavelength λ , we decompose the undulator length L into 3096 intervals corresponding to an element Δz of 1 mm. Any such interval corresponds to an element Δl on the beam path. In turn one has $\Delta l = r\Delta\theta$, where r is an instantaneous radius of curvature. In such a way, the sinusoidal positron trajectory is decomposed into elementary circular paths of variable radius r and variable aperture $\Delta\theta$. The photon flux emitted by positrons from any trajectory element Δl at position z can then be calculated by the standard formulas for a bending magnet which produces a magnetic field $B(z)$ as given in Eq. (1). The total photon flux will then be obtained by a suitable integration over z .

II.b) Calculation of photon flux for SIRLOIN

The number of photon $\Delta\Phi_B(A)$ emitted per milliradian angular path $\Delta\theta$ is given by:

$$\frac{\Delta\Phi_B(\lambda)}{\Delta\theta} = 2.457 \times 10^{13} E I y \int_y^\infty k_{2/3}(y') dy'. \quad (4)$$

Here E is the beam energy in GeV, I is the beam current in Ampere, $y = \lambda_c/\lambda$ (where λ_c is the critical frequency of synchrotron radiation) and $K_\nu(\lambda)$ is a modified, second-order Bessel function. Eq. (2) is then numerically evaluated under the assumption that the transverse displacement Δx of the point source in the undulator, being of the same order of magnitude as the beam width, may be neglected. The results are shown in Fig. 1 where the infrared photon flux Φ calculated for the SU3 undulator of Super ACO is compared with the one calculated for a bending magnet of the same ring. In the latter case, we assumed that radiation is extracted from a $\Delta\theta = 50$ mrad section of the orbit and is integrated in the vertical plane. The flux Φ emitted

by the undulator turns out to be greater by more than one order of magnitude at all wavelengths. The flux emitted by a 10 mm^2 black body at 2000 K under a solid angle of $50 \times 50 \text{ mrad}^2$, which can be considered as usual in conventional devices, is also shown for comparison. It should also be considered that globar sources in standard spectrophotometers are kept at temperatures ranging from 1300 to 1500 K.

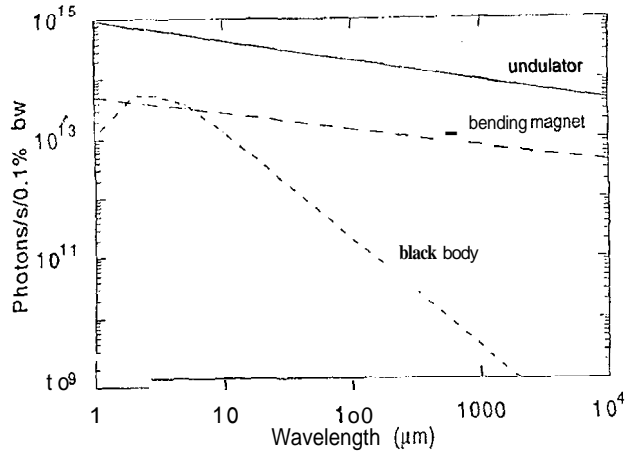


Figure 1: Infrared photon flux, as calculated for a 10 mm^2 black body at 2000 K under a solid angle of $50 \times 50 \text{ mrad}^2$ (dotted line), for IRSR produced by a bending magnet with $\text{AO} = 50 \text{ mrad}$ s (dashed line), and for IRSR emitted by the undulator SU3 with $K = 6.9$ (solid line) and a current of 200 mA injected.

The geometrical distribution of the radiation intensity, as effectively available at the extraction mirrors of SIRLOIN after taking into account the geometrical constraint of the undulator, is pictorially represented for a wavelength of $100 \mu\text{m}$ in Fig. 2 therein, each darker tone of grey corresponds to an intensity loss of 12,5% compared to its maximum value (white). The dotted lines represent the plane mirrors with a standard separation of 25 mm. They allow to evaluate the fraction of photon flux which is intercepted and transmitted to the line. Such fraction turns out to be about 80% in Fig. 2 and reduces to about 30% for a wavelength of $1 \mu\text{m}$. It can be noted in Fig. 2 that the infrared intensity presents a minimum at the centre of the ring, which makes the geometry here employed particularly suitable for the extraction of IRSR.

In fig. 3, the calculated photon flux being intercepted by the plane mirrors of SIRLOIN is plotted as a function of the radiation wavelength for different values of Δ . For comparison, the flux emitted^[6] by a black

body at 2000 K is also shown. Finally, we remark that even better performances would be obtained if the undulator were expressly designed for IRSR.

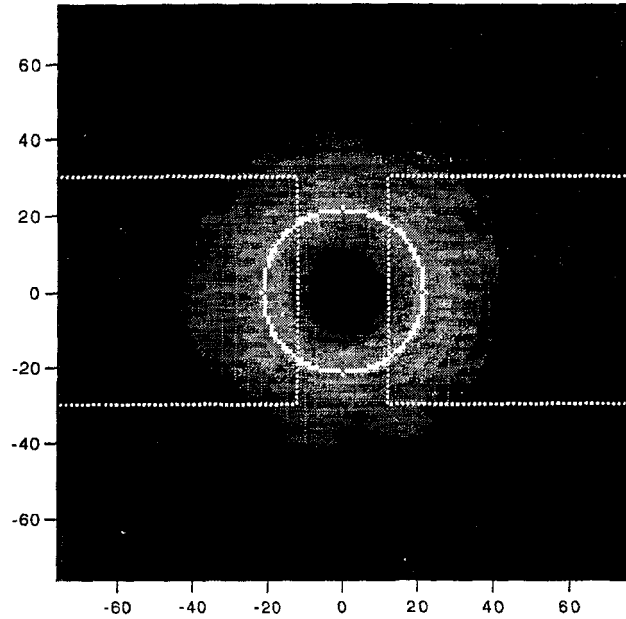


Figure 2: Distribution of the photon flux on mirrors M_1 and M_1' (represented by the dotted lines with scales in millimeters) at a wavelength of $100 \mu\text{m}$ and for a typical gap $\Delta = 25 \text{ mm}$. Each tone of gray from white to black corresponds to a 12,5% loss with respect to the maximum intensity.

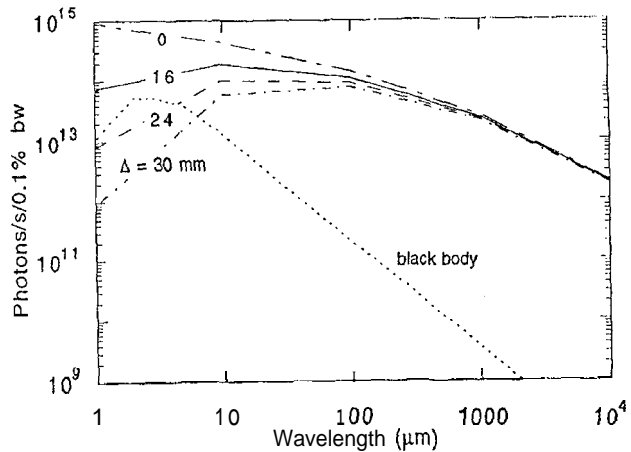


Figure 3: Intensity of the photon flux intercepted by the mirrors at the exit of the undulator SU3 of Super Aco, as calculated for various mirror separations Δ and compared to the emission of a black body (10 mm^2 black body at 2000 K collected under a solid angle of $50 \times 50 \text{ mrad}^2$).

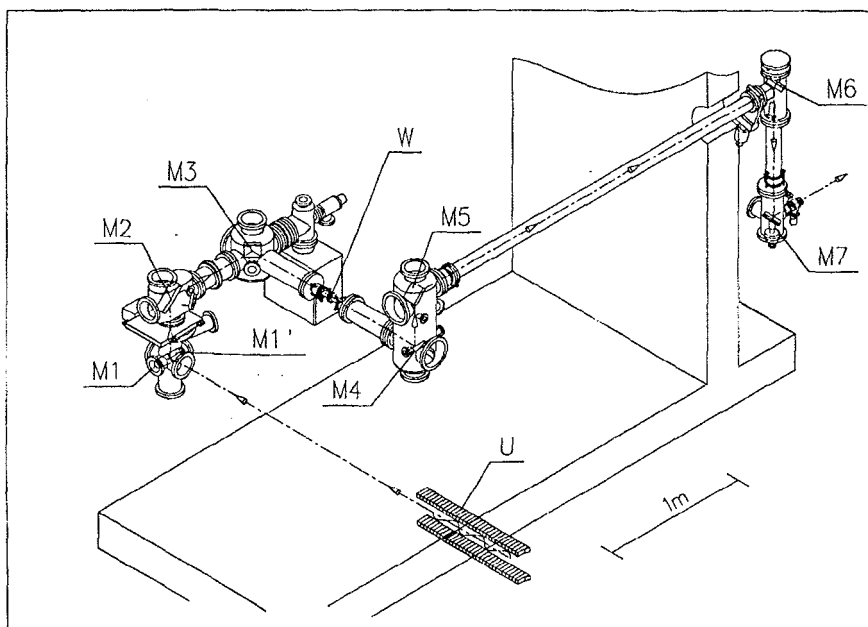


Figure 4: Schematic view of SIRLOIN, the IRSR line which is presently being assembled on the Super Aco storage ring of LURE. Wide-angle, low energy radiation produced by positrons in the undulator U is reflected vertically by plane mirrors M_1 and M_1' while the positrons and the hard part of the spectrum passes in between. The beam is then focussed by the cylindrical mirrors M_2 and M_3 on the diamond window W, and matched to the entrance optics of the interferometer by mirrors M_4 to M_7 . The diamond window W, which has an aperture of 1 cm, separates the ultrahigh-vacuum section of the line from the low vacuum of the interferometer.

III. The SIRLOIN spectroscopic system

The SIRLOIN beamline is schematically shown in Fig. 4. Its extracting mirror is assembled on one of the eight straight sections of the Super ACO storage ring, which contains the variable-gap undulator SU3 (U in Fig. 4). This latter has a length $L = 3096$ mm, a maximum $B_0 = 0.57$ T, and a magnet period $\lambda_0 = 12.9$ cm. The undulator is currently used in the wiggler mode, with B_0 corresponding to $K = 6.9$ for the 800 MeV positron energy^[8].

In the following description of the optical system, the source point is considered as being the centre of the undulator. However it is clear that the positrons, which emit photons through all their 3 meter trajectory in the undulator, cannot be considered as a point source. This remark holds for any synchrotron line for which a large collecting angle is involved.

At about 1 m from the output of the undulator two gold-coated, copper plane mirrors (M_1, M_1') are placed at 4° with respect to the z axis. The mirrors are water-cooled and are kept at a certain separation A in order to let positrons, X, and UV radiation pass through.

In such a way the IR beamline does not interfere with the existing ones, and in standard conditions the beam lifetime is not appreciably affected. Moreover, it is desirable to set the mirror separation A at its maximum value during the injection of positrons into the ring, when the beam is scarcely collimated. The mirror displacements are performed by a remote-controlled device. It is designed to move either mirror horizontally while keeping both parallel within a few milliradians, and while keeping the pressure in the ring at 5×10^{-11} torr. Such requirements have been fulfilled during the tests^[6].

Infrared and visible radiation is then focused onto the type 2A natural diamond window W by cylindrical mirrors M_2 and M_3 , which have their axes in the horizontal and vertical planes, respectively. The window is 200 microns thick, has a usable diameter of 10 mm and is wedged. The window separates the ultrahigh vacuum zone from the remainder of the line, which is equipped with plane (M_5 and M_6) and toroidal (M_4, M_7) mirrors. This section is kept at $\approx 10^{-3}$ torr in order to strongly reduce the infrared absorption due to water and CO_2 . The line ends in correspondence with the

"emission" port of a rapid scanning Bomem DA8 3X interferometer. The centre of the undulator (considered as the source point) is focalized on the last toroidal mirror M_7 while the M_1 extraction mirrors (considered as collimators) are focused onto the 10 mm entrance port of the interferometer. From there on, synchrotron radiation follows exactly the same optical path as the internal sources of the interferometer. This will allow a direct comparison of the intensity and brightness of IRSR with the well known equivalent quantities which can be measured from a black body.

IV. Some applications of IRSR to solid state physics

IVa. Studies on inorganic and ionic crystals at high pressures

Infrared synchrotron radiation has been successfully used for: performing high-pressure measurements in a diamond anvil cell (DAC) in Okasaki^[9] and in Brookhaven^[10]. Such experiments are difficult with conventional light sources, because of the small size of the windows.

Nanba and Watanabe^[11] measured the change in the optical phonon spectrum of a KI crystal in the 10-250 cm^{-1} range for the transverse optical phonon (TO). The variation in frequency ε as pressure p increases (Fig. 5) allows to calculate the Gruneisen parameter

$$\gamma = (d\varepsilon/dp)_T / k_T \varepsilon, \quad (5)$$

where k_T is the isothermal compressibility. γ is critically dependent on the shape of the repulsive part of the interatomic potential. Its spectroscopic measurement can be usefully compared to thermodynamic or macroscopic determinations, and provides detailed information on the potential at the atomic scale. In the KI system, a phase transition at 1.8 GPa from the rock salt structure to the caesium chloride has been observed by Nanba et al. using IRSR at the UVSOR^[11].

Phase transitions are also found in molecular crystals at high pressures^[12]. An example is given by solid CH_4 , where at least five phases have been observed, for which the orientational and/or the crystal structure differ. The corresponding changes in the Gruneisen parameter can be monitored in diamond anvil cell by IRSR absorption. One should notice that determinations of the Gruneisen parameter are also crucial in the assignment of the observed propagating modes in

molecular crystals. In general, translational phonons present γ values considerably higher than vibrational modes^[13].

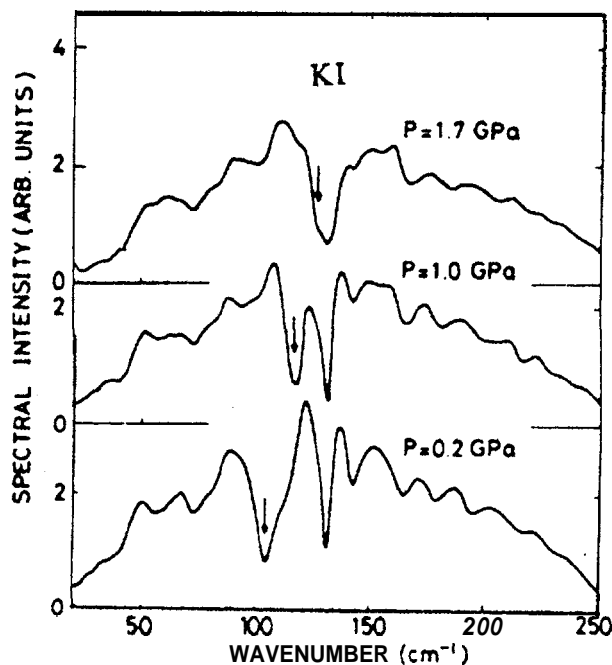


Figure 5: Transmission spectra of KI evaporated film of 2 μm thickness measured at room temperature under high-pressure using a diamond anvil cell. The pressures monitored by the energy shifts of the R1 fluorescence line of ruby are shown on spectra. Sharp dip structure due to the absorption of the TO phonon mode of KI crystal are shown by downward arrows. Structure at 130 cm^{-1} is due to the absorption of the crystalline quartz filter of the detector (from reference 9).

More recently Hanfland et al.^[10] also used synchrotron radiation for measurements of infrared spectra of samples at ultrahigh pressures. The measurements of vibrational transitions of solid hydrogen up to 180 megabar pressure revealed the mechanism for weakening the intramolecular interactions and strengthening the intermolecular interactions.

Although some of the above measurements could be accessed by Raman spectroscopy, their interpretation in IR spectra is more straightforward as they are not complicated by interference from visible absorption and fluorescence of the stressed diamond anvils. Moreover, in crystals where a centre of inversion is present, Raman active phonons are not infrared active and vice versa. As far as molecular vibrations are concerned, they are active in both kinds of spectra, but infrared absorption often provides better signal/noise ratios^[10].

IVb. Optical study of insulator-metal transition in semiconductors

Doped semiconductors represent an ideal system of hydrogenic atoms with one electron per site in which the transition from an insulating to a metallic state can be studied by varying the concentration of impurities. The change in the behaviour of electrons, which pass from localized to itinerant states, can be suitably monitored by optical spectroscopy in the far infrared. An example of a host system is Si, which presents characteristics of high purity. When increasing the impurity concentration, the absorption spectra change from a series of sharp lines into a unique broad band typical of metallic state. In order to refine the theoretical models one should study samples with concentrations as close as possible to the metallic concentration. This implies the needs of a more intense far infrared source than the conventional ones used for the previous studies and bright enough to overcome the limitations due to the small sample dimensions and reduced transmittance^[14].

IVc. Investigation of the anomalous Drude behavior of HTS

It is well known^[15,16] that the complex dielectric function $\epsilon(\omega)$ of High- T_c superconductors (HTS) in the normal-state ($T \geq T_c$ where T_c is the superconducting critical temperature) does not follow the ordinary Drude law

$$\bar{\epsilon}(\omega) = \epsilon_1 + i\epsilon_2 = \epsilon_\infty - \frac{\omega_p^2}{\omega^2 + i\omega\Gamma_D} \quad (6)$$

Here ϵ_1 includes all transitions at higher energies, while the Drude term includes plasma frequency ω_p and width Γ_D .

Infrared studies on single crystals belonging to different families of HTCS^[17]: $\text{La}_{2-x}\text{Sr}_x\text{CuO}_4$, $\text{Nd}_{2-x}\text{Ce}_x\text{CuO}_{4-y}$, $\text{Pb}_2\text{Sr}_2(\text{Eu,Dy})\text{Cu}_3\text{O}_8$, $\text{Bi}_2\text{Sr}_2\text{Ca}_n\text{Cu}_{n+1}\text{O}_{2n+4}$, $\text{YBa}_2\text{Cu}_3\text{O}_{7-y}$ have shown that Eq. (6) does not fully describe their spectra in the normal phase, as an extra-Drude absorption is always observed in the mid-infrared. Two different phenomenological approaches have been used to describe this effect. In the former approach, the optical conductivity $\sigma(\omega) = (\omega/4\pi)\epsilon_2$ at $\omega < 1$ eV is modeled by a "pseudo-Drude" term where both the effective mass of the carriers and their scattering rate depend on ω . Among the possible interpretations, incoherent scattering in a Marginal Fermi Liquid^[18], has been proposed.

According to an alternative approach, the dielectric function $\epsilon(\omega \leq \omega_{gap})$ is decomposed into an "ordinary Drude" term (where all parameters are independent of frequency) plus an extra-Drude term modeled by one or more Lorentz oscillators centered in the mid-infrared (MIR band):

$$\bar{\epsilon}(\omega) = \epsilon_\infty - \frac{\omega_p^2}{\omega^2 + i\omega\Gamma_D} + \frac{S_{\text{MIR}}^2}{(\omega_{\text{MIR}}^2 - \omega^2) - i\omega\Gamma_{\text{MIR}}}. \quad (7)$$

The MIR independent contribution in Eq.(7) could be due to interband transitions or to polaronic effects. In any case, the understanding of such extra-Drude absorption may provide important hints on the comprehension of the mechanism of superconductivity in HTCS. As a preliminary indication, recent infrared measurements have pointed out a connection between this anomaly and the critical temperature of High- T_c cuprates^[17,19].

A suitable material for such studies is $\text{YBa}_2\text{Cu}_3\text{O}_{7-y}$ (YBCO), where single crystals with high reflectivities, high critical temperatures, and intense Drude terms are commonly obtained. Nevertheless, in such samples the main part of the surface presents twinned crystals, which in turn cause ambiguities in the interpretation of physical information. Untwinned crystals are presently available only in very small sizes (typically $100 \times 100 \mu\text{m}^2$). Therefore the conclusions of recent studies by microscopic infrared spectroscopy are controversial. For instance, Rotter et al.^[20] find an extra-Drude absorption peaked at 0.25 eV cm^{-1} and assign it to the Cu-O chains of YBCO, while Koch et al.^[21] do not find any extra-Drude contribution from the chains and only observe a MIR band from Cu-O planes centred at 0.58 eV .

This type of studies is again a clear example of a situation where increased brightness would improve the reliability of experimental data. Another example is given by the investigation of the optical properties of single crystals along the c axis of the tetragonal structure. In this case, the difficulty is represented by the small thickness of most single crystals obtained up to now. Only $\text{La}_{2-x}\text{Sr}_x\text{CuO}_{4-y}$ single crystals, thick enough for accurate reflectivity measurements by conventional sources have been recently produced^[22], allowing the discovery of a superconducting phase along the c direction.

IVd. Determination of the superconducting gap in HTCS

According to the BCS theory in the weak-coupling approximation ($\lambda = N(E_f)U < 1$, where $N(E_f)$ is the density of electron states at the Fermi energy, and U is the average electron-phonon interaction), one has for the superconducting gap 2Δ the expression

$$2\Delta/kT_c = x \approx 3.5 \quad (8)$$

where T_c is the critical temperature. Larger values of x are predicted when strong-coupling corrections are introduced into the BCS theory. An unambiguous determination of the gap in High- T_c superconductors would then represent an important test for the theory, as it would inform whether: i) HTCS can be explained in the context of the BCS theory, ii) if yes, how strong the electron-phonon coupling may be. Attempts of measuring Δ have been made from the beginnings both by infrared reflectivity and tunnel experiments, leading to contradictory results: indeed, x values scattering from 3 to 8 and even more, were reported in the literature.

In the far-infrared, the opening of a gap at $T < T_c$ corresponds to the appearance of an edge in the reflectivity $R(\omega)$ at a photon energy close to 2Δ . In real systems, two conditions have to be fulfilled in order to perform meaningful measurements: i) the sample must have $R(\omega) = 1$ for $\omega \rightarrow 0$ in the normal phase, ii) the sample must be in an intermediate situation between the so-called 'clean limit' and the 'dirty limit'^[16]. In such case one will observe $R(\omega) = 1$ for any $\omega < 2\Delta$, while for $\omega > 2\Delta$, $R(\omega)$ will follow a Drude behaviour.

Transmission measurements, even if are also subjected to constraints, are more straightforward. The quality of sample surface is not quite as critical. Moreover, the edge would correspond here to the transmittance changing from a zero value to a finite value, and does not imply the definition of an absolute reference as in the case of reflectivity measurements.

Thin films cannot be used for far-IR transmission measurements as phonon absorption from the substrate would mask any change in the transmittance related to the opening of a gap. On the other hand, free standing crystals have low transmittance (from 0.1 to 0.2) and limited size. High brilliance is then requested. Pioneering measurements of $\text{Bi}_2\text{Sr}_2\text{CaCu}_2\text{O}_x$ in the region of the gap by means of IRSR sources have been reported^[23], even if no gap opening has been evidenced for $T < T_c$ (Fig. 6).

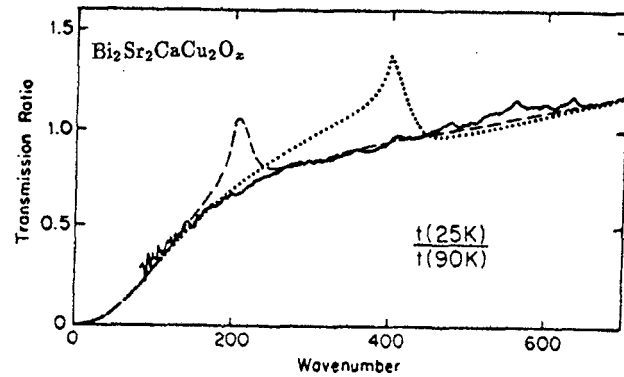


Figure 6: Ratio of the transmissions of $\text{Bi}_2\text{Sr}_2\text{CaCu}_2\text{O}_x$ at 25 and 90 K. The solid line represents the measured transmissions. The dashed and dotted lines were obtained from calculations. The Drude relaxation rate used was 50 cm^{-1} at 25 K. The BCS gap was assumed to be $2\Delta = 3.5 k_B T_c = 200 \text{ cm}^{-1}$. The calculation predicts a transmission peak even for $1/\tau < 2\Delta$, no peak is seen in the measurement (from reference 23).

V. Concluding remarks

The extraction system of SIRLOIN is new in its concept as for the first time the collecting mirrors are placed directly on the trajectory of the positrons themselves and as it allows two regions of the spectrum (the soft X-ray and the infrared) to be exploited in parallel. In this study two important questions concerning such a device have been answered. Firstly, how small can the gap between the two mirrors be before the positrons beam is significantly affected. Secondly, according to calculations what fraction of radiation can be collected in the infrared and far-infrared range.

It should be remembered that all the calculations are based on the assumption that coherence effects are negligible due either to the very large divergence and to the length of the source. We are currently developing a program that would allow to include such effects. Another desirable improvement would be the calculation of the degree of polarisation of the light.

Moreover, measurements of the infrared intensity as compared to the radiation emitted by a black body source is being completed. This will allow in turn a comparison to the calculated intensity. This comparison extended for different values of the undulator parameter K and for different gap values should allow a deeper understanding of the undulator emission for longer wavelengths. After the optimization of the optical system the scientific program will then start with

emphasis on experiment for which synchrotron radiation brightness and intensity may provide information that could not be accessed with conventional sources.

Acknowledgements

The development of this beam line was only possible in close collaboration with the technical staff of the LURE facility, the authors are sincerely grateful to them. We also acknowledge the strong support and encouragement from the direction of LURE.

We also thank gratefully J. M. Ortega, H. Zyn-gier, C. Jacobsen, G. Williams, K.-J. Kim, H. Szwarc, M. Capizzi and P. Marin for stimulating discussions and advice. This work was supported in part by the Chemistry Department of CNRS, the Ministry of Research and Technology, the CPMA and the Institut de Physique Moléculaire at Université d'Orsay. One of us (P.C.) wishes to thank the CNRS for a senior visiting fellowship at LURE.

References

1. G. P. Williams, Nucl. Instr. and Meth. **A291**, 8 (1990).
2. T. Nanba, J. Yarwood, T. Shuttleworth, and J. E. Hasted, Int. J. Infrared & MM Waves **7**, 759 (1986).
3. M. Hara, S. H. Be, I. Taliesliita and T. Nanba, Rev. Sci. Instrum. **63**, 1543 (1992).
4. D. A. Slater, P. Hollins, M. A. Chesters, J. Pritchard, D. H. Martin, M. Surman, D. A. Shaw, I. Munro, Rev. Sci. Instrum. **63**, 1547 (1992).
5. Max Lab activity report 1991, National Laboratory Lund, Sweden.
6. P. Roy, Y. L. Mathis, A. Gerschel, J. P. Marx, J. Michaut, B. Lagarde and P. Calvani, Nucl. Instr. and Meth. **A325**, 568 (1993).
7. S. Krinski, W. Thomlinson, A. Van Steenberg, Internal report, Brookhaven National Laboratory 31080, **3** (1982).
8. M. Barthès, C. Bazin, M. E. Couprie, A. Dael, C. Evesque and C. Humbert, Internal report, Super Aco/87-63, (1987).
9. T. Nanba, Rev. Sci. Instr. **60**, 1680 (1989).
10. R. Hanfland, R. J. Hemley, H. K. Mao and G. P. Williams, Phys. Rev. Lett. **69**, 1129 (1992).
11. T. Nanba and T. Watanabe, J. Phys. Soc. Jpn. **58**, 1535 (1989).
12. M. M. Thiéry, D. Fabre and K. Kobashi, J. Chem. Phys. **83**, 6165 (1985).
13. F. D. Medina, J. Chem. Phys. **73**, 77 (1980).
14. G. A. Thomas, M. Capizzi, F. De Rosa, R. N. Bliatt and T. M. Rice, Phys. Rev. **B23**, 5472 (1981).
15. P. B. Allen, to be published.
16. T. Timusk and D. B. Tanner, *Infrared properties of High Tc Superconductors, in Physical Properties of High Temperature Superconductors*, ed. by D. M. Ginsberg, (World Scientific), Singapore, (1989).
17. P. Calvani, M. Capizzi, P. Dore, S. Lupi, P. Maselli, G. Paleologo, G. Balestrino, M. Marinelli, E. Milani, H. Gerger, P. Roy and Y. L. Mathis, Int. J. Infrared & MM. Waves in press.
18. C. M. Varma, P. B. Littlewood, S. Schmitt-Rink, E. Abrahams and A. E. Rukenstein, Phys. Rev. Lett. **63**, 1996 (1989); Physica **C135**, 152 (1990).
19. P. Calvani and S. Lupi, Solid State Commun., **85**, 665 (1993).
20. L. D. Rotter, Z. Schlesinger, R. T. Collins, F. Holtzberg, C. Field, U. W. Welp, G. W. Crabtree, J. Z. Liu, Y. Fang, K. G. Vandervoort and S. Fleshler, Phys. Rev. Lett. **67**, 2741 (1991).
21. B. Koch, H. P. Geserich and T. H. Wolf, Solid State Commun. **71**, 495 (1989).
22. T. Timusk, D. A. Bonn, J. E. Greedan, C. V. Stager, J. D. Garrett, A. H. O'Reilly, M. Reedik, K. Kamaras, C. D. Porter, S. L. Herr and D. B. Tanner, Physica **C 152-155**, 1744 (1988).
23. L. Forro, G. L. Carr, G. P. Williams, D. Mandrus and L. Mihaly, Phys. Rev. Lett. **65**, 1941 (1990).